EIGHTH EUROPEAN ROTORCRAFT FORUM

Paper No. 10.2

A SIMPLE SYSTEM FOR HELICOPTER INDIVIDUAL-BLADE-CONTROL AND ITS APPLICATION TO LAG DAMPING AUGMENTATION

Norman D. Ham

Brigitte L. Behal

Robert M. McKillip, Jr.

M.I.T., U.S.A.

August 31 through September 3, 1982

AIX-EN-PROVENCE, FRANCE

ASSOCIATION AERONAUTIQUE ET ASTRONAUTIQUE DE FRANCE

A SIMPLE SYSTEM FOR HELICOPTER INDIVIDUAL-BLADE-CONTROL AND ITS APPLICATION TO LAG DAMPING AUGMENTATION

Norman D. Ham*
Brigitte L. Behal**
Robert M. McKillip, Jr.**

Department of Aeronautics and Astronautics
Massachusetts Institute of Technology
Cambridge, Massachusetts 02139

Abstract

A new, advanced type of active control for helicopters and its application to a system for blade lag damping augmentation is described.

The system, based on previously developed M.I.T. Individual-Blade-Control hardware, employs blade-mounted accelerometers to sense blade lag motion and feeds back rate information to increase the damping of the first lag mode. A linear model of the blade and control system dynamics is used to give guidance in the design process as well as to aid in analysis of experimental results. System performance in wind tunnel tests is described, and evidence is given of the system's ability to provide substantial additional damping to blade lag motion.

1. Introduction

A truly advanced helicopter rotor must operate in a severe aerodynamic environment with high reliability and low maintenance requirements. This environment includes:

(1) atmospheric turbulence (leading to impaired flying qualities, particularly in the case of hingeless rotor helicopters).

(2) retreating blade stall (leading to large torsional loads in blade structure and control system).

(3) blade-vortex interaction in transitional and nap-of-the-earth flight (leading to unacceptable higher harmonic blade bending stresses and helicopter vibration).

(4) blade-fuselage interference (leading to unacceptable higher harmonic blade bending stresses and helicopter vibration).

(5) blade instabilities due to flap-lag coupling and high advance ratio (including blade "sailing" during shut-down).

The application of feedback techniques make it possible to alleviate the effects described in items (1) to (5) above, while improving helicopter vibration and handling characteristics to meet desired standards. The concept of Individual-Blade-Control (IBC) embodies the control of broadband electrohydraulic actuators attached to each blade, using signals from sensors mounted on the blades to supply appropriate control commands to the actuators[1-5]. Note that the IBC involves not just control of each blade independently, but also a feedback loop for each blade in the rotating frame. In this manner it becomes possible to reduce the severe effects of atmospheric turbulence, retreating blade stall, blade-vortex interaction, blade-fuselage interference, and blade instabilities, while providing improved flying qualities and automatic blade tracking.

It is evident that the IBC system will be most effective if it is comprised of several subsystems, each controlling a specific mode, e.g., the blade flapping mode, the first blade lag mode, the first blade flatwise bending mode, and the first blade torsion mode. Each sub-system operates in its appropriate frequency band.

The configuration used in this investigation employs an individual actuator and multiple feedback loops to control each blade. These actuators and feedback loops rotate with the blades and, therefore, a conventional swash plate is not required. However, the same degree of individual-blade-control can be achieved by placing the actuators in the non-rotating system and controlling the blades through a conventional swash plate if the number of control degrees-of-freedom equals the number of blades. For more than three blades, the use of extensible blade pitch control rods in the form of hydraulic actuators is a possibility. See Ref. 5 for some other design solutions.

The present paper is concerned with the application of the Individual-Blade-Control concept to blade lag damping augmentation. To achieve this, a servomotor controls the pitch angle of the blade whose lag acceleration is sensed by two accelerometers, and an integrator yields the lag velocity which is fed back through a compensator to the blade pitch control. A blade flapping

This research was sponsored by the Ames Research Center, NASA, Moffett Field, California 94035. Major contributions to the project were made by P.H. Bauer.

*Director, VTOL Technology Laboratory.
**Research Engineers.

velocity is thus generated which in the presence of blade coning angle, results in an in-plane moment due to Coriolis forces which opposes lag motion and is proportional to lag velocity, i.e., blade lag damping is augmented.

The theoretical model is described in Section 2, and lag rate signal extraction is outlined in Section 3. A classical control analysis is used to design an appropriate compensator for the wind tunnel model in Section 4 and for a full size blade in Section 5. The wind tunnel model is described in Section 6. Then, a series of tests, whose results are given in Section 7, was run in the wind tunnel. Finally, conclusions are presented in Section 8.

Further details are given in Reference 6.

2. Theoretical Analysis

This section derives the equations of motion of the blade neglecting the cross-coupling between lag and flapping dynamics.

Figure 1 shows an inplane view of the articulated offset hinged rotor blade where a_L is the lag acceleration and is equal to:

$$a_L = a_{L_1} + a_{L_2} \tag{1}$$

According to Figure 1; we can write:

$$\varepsilon = \zeta - \delta$$
$$r\varepsilon = (r-e)\zeta \tag{2}$$

$$\delta = \frac{e}{r}\zeta \tag{3}$$

$$a_{L_2} = (r-e)\ddot{\zeta}$$

Assuming the angles are small, a_{L_1} can be computed from (3)

$$a_{L_1} = r\Omega^2 \sin\delta = r\Omega^2\delta = \Omega^2\zeta e \tag{4}$$

Substitution of a_{L_1} and a_{L_2} in Equation (1) gives

$$a_L = (r-e)\ddot{\zeta} + \Omega^2 e\zeta \tag{5}$$

The equation of motion is obtained by summing moments about the lag hinge:

$$\Sigma M = M_C + M_I = 0 \tag{6}$$

where

M_C = Coriolis moment = $-\int_e^R 2(r-e)^2\Omega\beta\dot{\beta}\, mdr$

M_I = lag inertial moment = $-\int_e^R a_L(r-e)mdr$

Substitution of M_C and M_I in Equation (6) yields,

$$\ddot{\zeta}\int_e^R m(r-e)^2dr + \zeta\int_e^R(r-e)\Omega^2 emdr = 2\beta\dot{\beta}\int_e^R m(d-e)$$

(7)

Define $I_L = \int_e^R m(r-e)^2dr$ = moment of inertia abo the lag hinge

$$\omega_L^2 = \frac{m\Omega^2 e\int_e^R(r-e)dr}{I_L} = \text{natural lag frequenc of the blade}$$

Introducing these quantities in Equation (7) and factoring I_L gives Equation (8)

$$\ddot{\zeta} + \omega_L^2\zeta = -2\Omega\dot{\beta}\beta \tag{8}$$

where $\beta = \beta_0 + \beta_{1c}\cos\psi + \beta_{1s}\sin\psi$

and $\beta_{1c}\cos\psi$ and $\beta_{1s}\sin\psi$ are neglected with respect to the steady state component β_0, which implies that

$$\beta\dot{\beta} \approx \beta_0\dot{\beta}$$

The Laplace transform applied to Equation (8) yields the lag transfer function with respect to the flapping velocity,

$$H(s) = \frac{\zeta(s)}{\dot{\beta}(s)} = -\frac{2\Omega\beta_0}{s^2+\omega_L^2} \tag{9}$$

The well known flapping equation of motion for a blade with offset flapping hinge is

$$I_1\ddot{\beta} + m\int_e^R r(r-e)\Omega^2\beta dr = \frac{1}{2}\rho ac\Omega^2\int_e^R(r-e)r\cdot$$
$$[\theta r - (r-e)\frac{\dot{\beta}}{\Omega}]dr \tag{10}$$

where

$$I_1 = m\int_e^R(r-e)^2dr = \frac{m}{3}(R-e)^3$$

and neglecting inflow for present purposes.

In order to avoid tedious expressions, e an R, which are fixed values for the model, are replaced by their numerical values in Equation (10). After simplification and reordering, we obtain

$$\ddot{\beta} + 0.79\frac{\gamma}{8}\Omega\dot{\beta} + 1.13\,\Omega^2\beta = 0.89\frac{\gamma}{8}\Omega^2\theta \tag{11}$$

The Laplace transform applied to Equation (11) gives the flapping transfer function with respec to the pitch angle:

$$G(s) = \frac{\dot{\beta}(s)}{\theta(s)} = \frac{.098\,\gamma s}{\frac{s^2}{1.13\Omega^2} + \frac{0.79}{1.13\Omega}\frac{\gamma}{8}s+1} \tag{12}$$

3. Lag Rate Signal Extraction

In order to build a compensator increasing the lag damping of the rotor blade, it is necessary to extract the lag rate. The output signals of two inplane accelerometers, one at the tip and the other at midspan of the blade, are subtracted to give a pure lag acceleration which is then fed back to an integrator in order to get the lag rate.

The accelerometers sense the lag acceleration $a_L = a_{L_1} + a_{L_2}$. As shown in Section 2, a_{L_1} which is the centrifugal acceleration, does not depend on the position of the accelerometers on the blade: a_{L_2} is directly proportional to the distance between the lag hinge and the accelerometer.

The signal sensed by the mid-span is:

$$a_L = \frac{1}{2}(R-e)\ddot{\zeta} + \Omega^2\zeta e \qquad (13)$$

Similarly, the tip accelerometer senses:

$$a_L = (R-e)\ddot{\zeta} + \Omega^2\zeta e \qquad (14)$$

Subtracting Equation (13) from Equation (14) yields the lag acceleration

$$a_L = \frac{1}{2}(R-e)\ddot{\zeta} \qquad (15)$$

Applying the Laplace transform to Equation (15) gives the accelerometer transfer function

$$A(s) = \frac{1}{2}(R-e)s^2 = 0.93\ s^2$$

Integration of this signal yields blade lag rate. Unfortunately, an ideal integrator would apply an infinite d.c. gain to the steady-state component in the lag signal; to solve this problem, an integrator with a roll-off frequency of 7 rad/s was designed, as described in the Appendix.

4. Design of the Compensator

The design of the compensator is based on the root locus of the overall system, composed of a servomotor controlling the pitch motion of the blade, which is equipped with two accelerometers, whose output is fed into an integrator.

Equations (9) and (12) give the lag and flapping transfer functions. The integrator transfer function can be found in the Appendix, and the accelerometer transfer function is given in Section 3.

From the block diagram given in Figure 2, the closed loop transfer function from V to ζ with no compensation has no value of K_R for which the system is stable, and it is necessary to compensate the fourth zero which drives the system unstable (see Figure 2). A simple way of achieving this, according to the classical theory, is to add a pole close to the zero: this approach yields a compensator, the transfer function of which is

$$D(s) = \frac{-4.16}{\left(\frac{s}{0.24} + 1\right)}$$

The physical realization of this compensator is presented in the Appendix.

According to the block diagram given in Figure 2, the closed loop transfer function from V to ζ is then

$$H(s) = \frac{-2.3\times10^{-3}\, s\ (s/0.24 + 1)(s/7 + 1)^2}{\left(\frac{s^2}{18\times10^4} + \frac{s}{300} + 1\right)\left(\frac{s^2}{1.13\Omega^2} + \frac{0.79}{1.13\Omega}\,\chi\, s + 1\right)\left(\frac{s^2}{\omega_L^2} + 1\right)\left(\frac{s}{0.24} + 1\right)\left(\frac{s}{7} + 1\right)^2 + 3\times K_R\times10^{-4}}$$

A plot of the root locus is given in Figure 3. We can see that the compensator has stabilized the system. The circled crosses indicate the location of the poles for the design value of the gain. The open loop sensitivity is $S = 1.2\times10^{-3}$. It implies a gain K_R equal to $S = 3\times10^{-4}=4$.

Figure 4 shows the open and closed loop Bode plots from V to ζ: the lag damping ratio has been increased, while the flapping damping ratio has been reduced.

5. Application to a Full-Size Blade

The theoretical analysis and the design of the compensator have been based on the model blade used in the wind tunnel tests. In the previous theoretical analysis, this model mainly differs from a full-size blade by its Lock number; a full size blade would have a Lock number of about 8 instead of 3. To extend the results to the real case, a root locus analysis has been made with $\gamma = 8$ and the same compensator. The plot of the root locus, given in Figure 5, shows that, in the case of the full-size blade, it is possible to increase the lag damping ratio up to 0.46. The corresponding flap damping ratio is 0.15. The circled crosses indicate the values of the poles for these damping ratios. The corresponding closed-loop sensitivity is equal to 3×10^{-3}.

Figure 6 shows the open-loop Bode plot of the system, and the closed-loop Bode plot for a closed-loop sensitivity of 3×10^{-3}. It is seen that the improvement is even more significant

with a full-size blade than with the model. This is due to the fact that the flapping damping ratio is proportional to the Lock number; there is a bigger margin to improve the lag damping ratio. The performance of the compensator remains acceptable with a full-size blade.

6. Model Design and Description

The model used here to test the proposed system was identical in most particulars to that used in Ref. 3. A D.C. servomotor acting as a blade pitch position control system was mounted on the rotor shaft. The test rotor used only a single blade, with a NACA 0012 section 21.2 inch span, and a two inch chord; further details of the blade are given in Table 1. The blade was attached to the rotor hub by means of a steel fork which in turn was connected to a spherical bearing; thus the blade's flapping, lagging, and feathering motions all took place about the same point. A steel flexure instrumented with strain gauges was attached to the blade to sense pitch angle.

Two "dummy blades" in the form of lengths of threaded 5/8" steel rod were also attached to the rotor hub. Each rod had adjustable counterweights which were used to achieve dynamic balancing during rotor operation. Two symmetrically mounted counterweights were also attached to the shaft to balance the active motor.

The blade and control system hardware are shown in Fig. 7. Further details of the construction of the actuation system are given in Ref. 3 and will not be repeated here.

7. Test Results and Discussion

Testing of the I.B.C. lag damping augmentation system was performed in the M.I.T. VTOL Wind Tunnel. The 10 ft x 12 ft test section contained two vertical trunnions which supported the rotor shaft in a horizontal attitude. This orientation, which caused the rotor to rotate in a vertical plane, was a result of the mounting requirements of the previous series of I.B.C. gust alleviation tests (Ref. 3). One consequence of this orientation was to introduce a one-per-rev gravity pulse into the accelerometers used in the lag control system.

The rotor was driven by an external hydraulic motor. The shaft was equipped with slip rings to provide power to the servomotor and to extract data from the various sensing elements. On-line data extraction was accomplished using software previously developed by other members of the I.B.C. project team.

The equipment used for the tests consisted of a portable analog computer and servo amplifier, for processing the feedback loop signals and driving the motor, a dual beam storage oscilloscope, for monitoring the lag and pitch signals, a function generator for providing the pitch actuation signal, and a P.D.P.-11 computer for analog-to-digital data acquisition and real-time Fast Fourier Transform analysis.

A series of tests was run with the rotor operating in hover at a rotational speed of 78.5 rad/s. It consisted of increasing the gain of the feedback loop step-by-step, and getting, for each gain value, a real-time trace and Fast Fourier Transform of the pitch input and the accelerometers' output.

The open loop time traces of the accelerometers' output shown in Fig. 8 had a one-per-rev gravity component that strongly affected the output signals. In addition, friction of the spherical bearing which acted as a lag hinge caused an unrealistically large amount of lag motion damping. Both these effects tended to obscure the incremental lag damping due to the control system.

In order to reduce the lag hinge friction, the rotor test rotational speed was reduced to 37.7 rad/sec. At this speed the open loop lag damping ratio, largely due to friction, was found to be 0.37.

A new series of wind tunnel tests was run at this rotational speed, utilizing white noise excitation of blade pitch. The results are shown in Fig. 9, in terms of lag acceleration magnitude and phase as a function of pitch excitation frequency for the rotor in hover and at advance ratio 0.27. (For details of the experimental method, see Ref. 7.)

The experimental lag acceleration response in Fig. 9 is seen to be relatively flat until lag resonance is approached near 14 rad/sec. This reduction in lag response is believed to be due to two separate aerodynamic effects (in addition to mechanical friction). The first was encountered in the tests described in Ref. 3. Dynamic inflow effects were found to reduce the flapping response to sinusoidal pitch input by as much as 65% in hover, and by 30% at advance ratio 0.3. Since lag motion in the present system is controlled by flapping-induced Coriolis forces, a reduction in flapping response to blade pitch input will reduce the associated blade lag response. The other adverse aerodynamic effect is shown in Ref. 8 to be a reduction in the flapping-induced Coriolis moment about the lag hinge by an associated and opposed induced drag moment. Neither aerodynamic effect was included in the present theory, and it appears that a truly quantitative analysis should include both effects. This refinement was not added to the present analysis due to the difficulty of including the equally important bearing friction in such a quantitative analysis.

The amplitude responses in Figs. 9(a) and 9(b) are inconclusive in demonstrating an increase in lag damping due to the control system. However the associated phase angle data are conclusive. Both figures show a rotation of the slope of the phase angle versus frequency curve at lag

resonance, in the direction of increased lag damping, as K_β is increased from zero to 3. The effect is more pronounced at advance ratio of 0.27 than at hover, possibly reflecting the reduction of the adverse dynamic inflow effects with advance ratio described above. The increase in lag damping ratio due to the control system was determined to be 0.18 in hover and 0.37 at advance ratio 0.27. These values are incremental to the open loop value of 0.37.

An improved experiment would require re-orientation of the rotor to a near-horizontal position to eliminate the lag gravity moment, and re-design of the present lag hinge to reduce mechanical friction.

8. Conclusions

From the preceding theoretical analyses and experiments, the following conclusions can be drawn:

(1) The concept of controlling lag damping via the Coriolis forces due to pitch-induced flapping was shown to be feasible.

(2) A simple linear model of blade and servomotor dynamics gave substantial guidance in the design of a simple damping augmentation system based on I.B.C. techniques.

(3) A quantitative theoretical analysis requires the inclusion of dynamic inflow effects on the flapping response to pitch input, and induced drag effects on the net moment about the lag hinge due to flapping velocity.

(4) No apparent fundamental obstacle exists to extending the control techniques developed to full-size rotors.

References

1. Kretz, M., "Research in Multicyclic and Active Control of Rotary Wings", Vertica, 1, 2, 1976.

2. Ham, N.D., "A Simple System for Helicopter Individual-Blade-Control Using Modal Decomposition", Vertica, 4, 1, 1980.

3. Ham, N.D. and McKillip, R.M. Jr., "A Simple System for Helicopter Individual-Blade-Control and Its Application to Gust Alleviation", Proc. Sixth European Rotorcraft Forum, Bristol, England, September 1980.

4. Ham, N.D. and Quackenbush, T.R., "A Simple System for Helicopter Individual-Blade-Control and Its Application to Stall-Induced Vibration Alleviation", Proc. AHS National Specialists' Meeting on Helicopter Vibration, Hartford, Connecticut, U.S.A., November 1981.

5. Guinn, K.F., "Individual Blade Control Independent of a Swash Plate", JAHS, 27, 3, July 1982.

6. Behal, Brigitte L., "Design and Testing of a Control System to Increase the Lag Damping of a Helicopter Blade", M.I.T. VTOL Technology Laboratory, TR-196-4, August 1982.

7. Johnson, W., "Development of a Transfer Function Method for Dynamic Stability Measurement", NASA TN D-8522, July 1977.

8. Blake, B.B. et al., "Recent Studies of the Pitch-Lag Instabilities of Articulated Rotors", JAHS, 6, 3, July 1961.

TABLE 1

DESCRIPTION OF THE ROTOR BLADE USED IN THE WIND TUNNEL TEST

No. of blades	1
Radius, R	2.031 ft
Chord, c	2 inches
Lift Curve slope, a	5.73
Collective pitch, $\theta_{0.75}$	8 deg
Lock number, γ	3.01
Hinge offset, e (flapping or lag)	2.0 inches
Section	NACA 0012
Aerodynamic center	25% chord
Pitch control axis	25% chord
Twist	-8°

NOMENCLATURE

c	Blade chord
s	Laplace operator
e	Lag hinge offset
m	Blade mass per unit of length
R	Rotor radius
ζ	Blade lag angle
θ	Pitch angle
Ω	Angular velocity of the rotor
γ	Lock number = $\frac{\rho a c R^4}{I_\zeta}$
β	Flapping angle

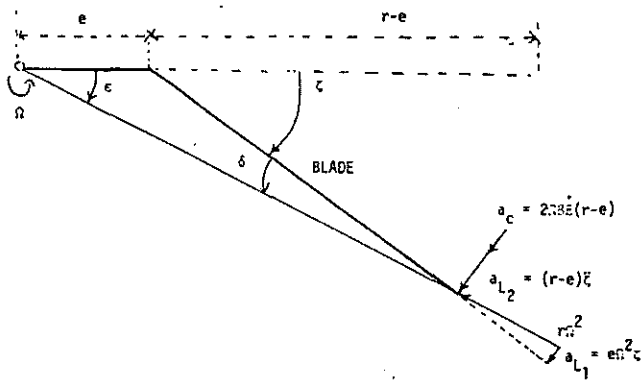

FIG. 1 Inplane View of the Blade

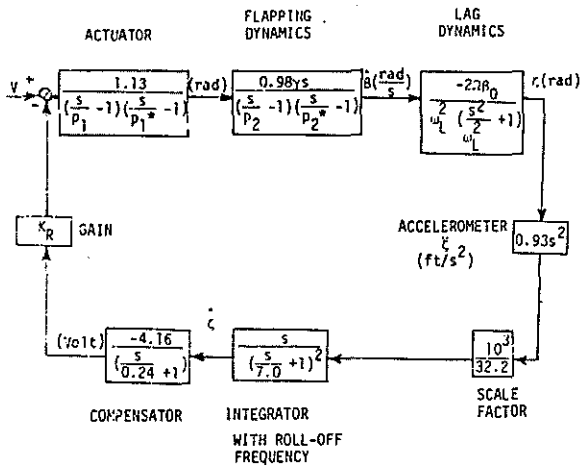

p_1 = -300(1+j)

p_2 = -12.1 + 82.57j

ω_L = 28.74 rd/s

FIG. 2 Block Diagram of the System with Compensator

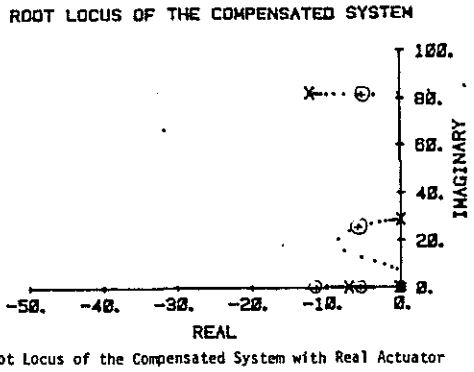

FIG. 3 Root Locus of the Compensated System with Real Actuator

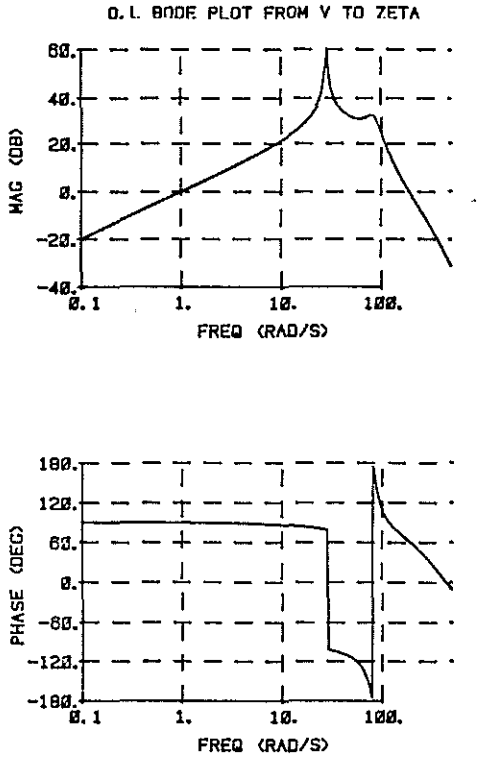

FIG. 4(a) Open Loop Bode Plot of the System from the Voltage Input to the Lag Angle

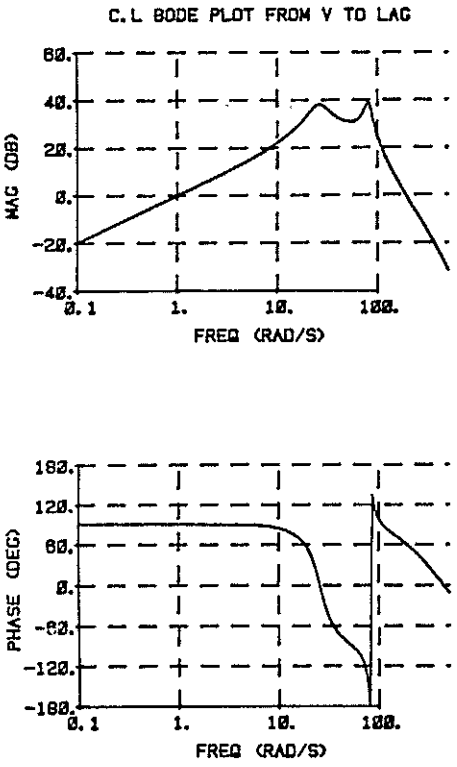

FIG. 4(b) Closed Loop Bode Plot of the Compensated System from Voltage Input to the Lag Angle, $K_R = 4$

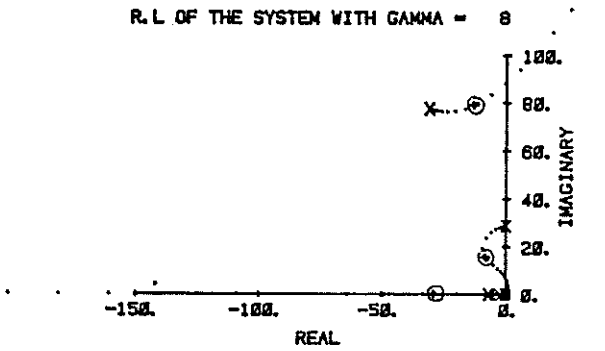

Open Loop Poles: $P_1 = \pm j \times 28.74$ Open Loop Zeroes: $z_1 = 0$

$P_2 = -31 \pm j \times 77.47$

FIG. 5 Root Locus of the System with Real Blade

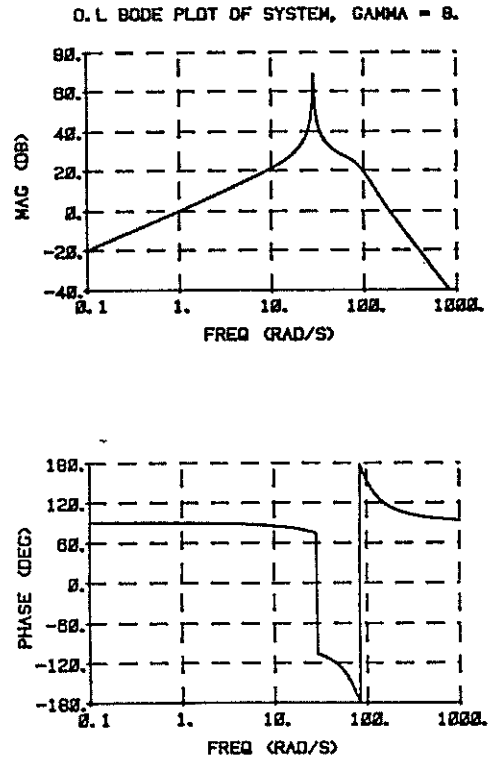

FIG. 6(a) Open Loop Bode Plot of the System with Real Blade from Input to Lag Angle

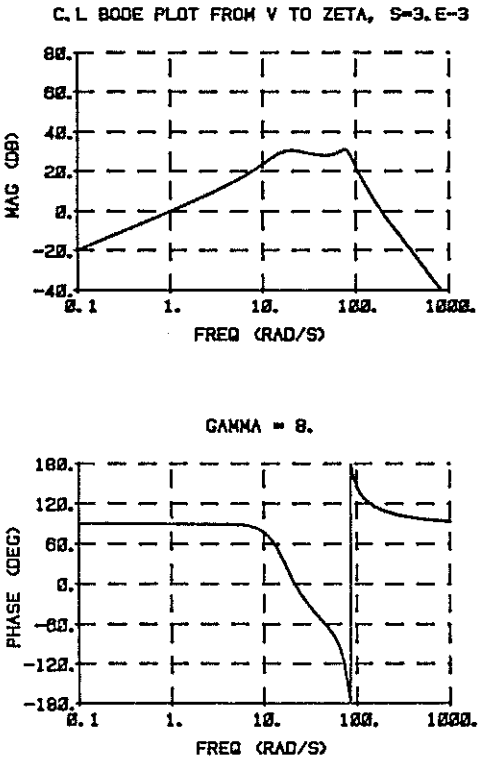

FIG. 6(b) Closed Loop Bode Plot of the System with Real Blade from Input to Lag Angle, $S_{OL} = 3 \times 10^{-3}$

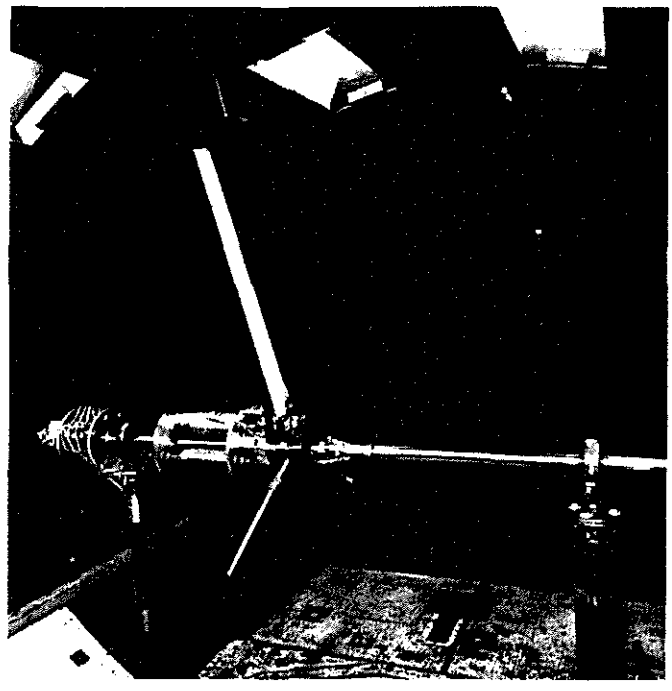

FIG. 7 Individual-Blade-Control Experimental Rig, Upstream View

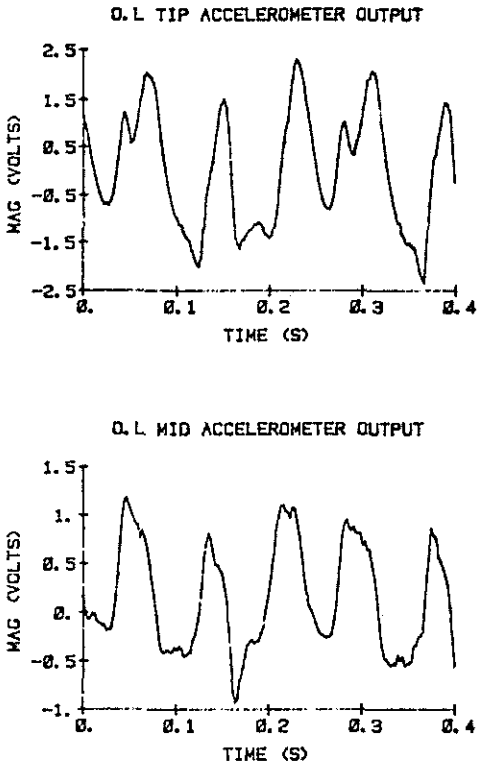

FIG. 8 Open-Loop Accelerometer Outputs, $\mu = 0$, $K_R = 0$, $\Omega = 78.5$ rad/s

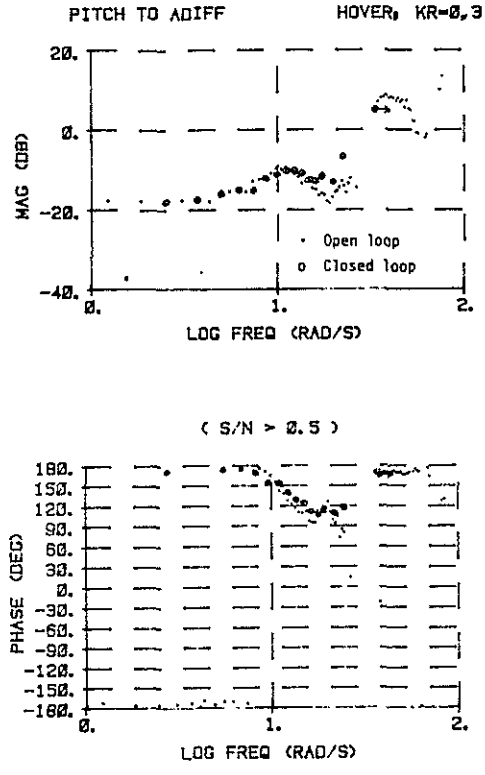

FIG. 9(a) Experimental Results, μ=0, Ω=37.7 rad/s. Pitch θ to Accelerometer Difference Signal 1/2 (R-e)ζ

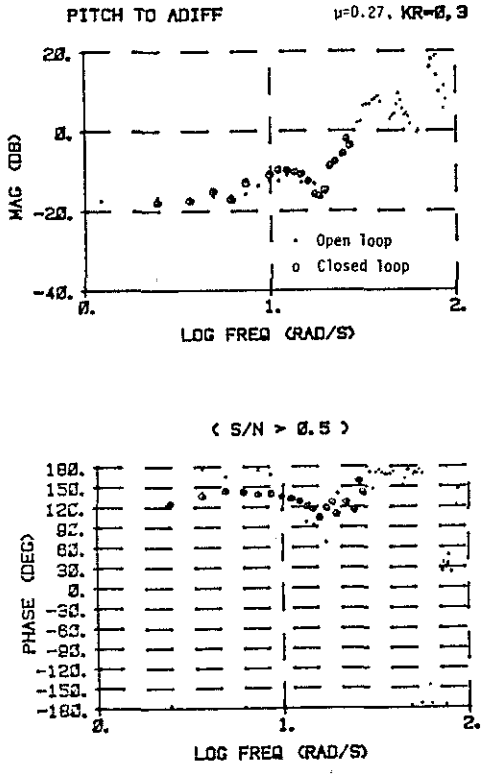

FIG. 9(b) Experimental Results, μ=0.27, Ω=37.7 rad/s. Pitch θ to Accelerometer Difference Signal 1/2 (R-e)ζ

APPENDIX

CONTROL BLOCK DESIGN

As noted in Section 3, the output signal of the mid-span accelerometer is subtracted from the output signal of the tip accelerometer, then fed to an integrator with a roll-off frequency of 7 rd/s, and then fed back through a compensator.

The integrator transfer function is

$$H(s) = \frac{s}{(s/7 + 1)^2}$$

and the compensator transfer function is given in Section 4:

$$D(s) = \frac{-4.16}{(s/0.24 + 1)}$$

For technical reasons, it was decided to design a block containing the subtracting operator, the integrator and the compensator as shown in Figure A.1.

The values of the components are

$R^1 = 9.3\ k\Omega$ $\quad R = 42.2\ k\Omega$

$R_1 = 832\ k\Omega$ $\quad C_2 = 1\mu F$

$R_2 = 143\ k\Omega$ $\quad C_1 = 5\mu F$

A theoretical analysis of the block integrator and compensator has been made and an open-loop Bode plot of this system is given in Figure A.2. It can be compared with the experimental response of the real system given in Figure A.3: they match very well.

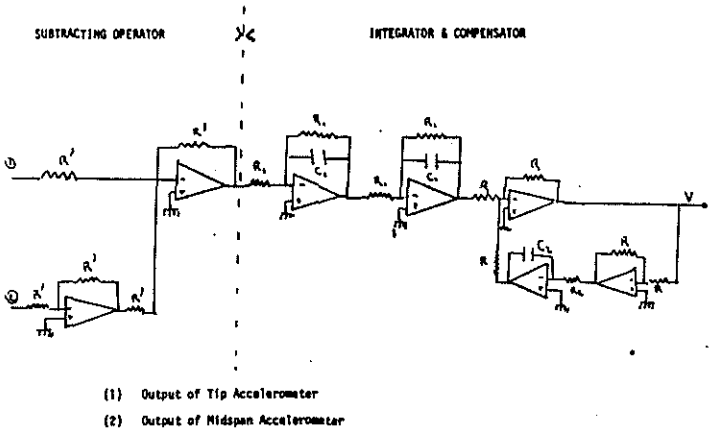

FIG. A.1 Control Block with Subtracting Operator, Integrator and Compensator

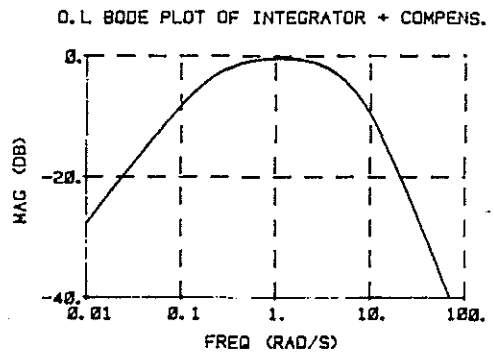

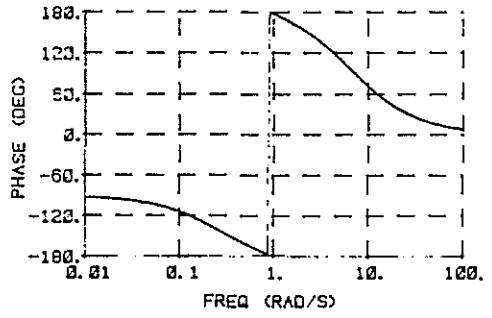

FIG. A.2 Open Loop Bode Plot of Integrator and Compensator

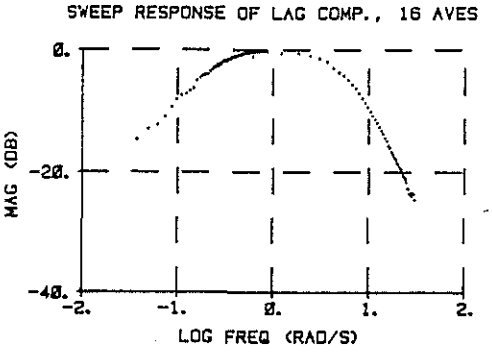

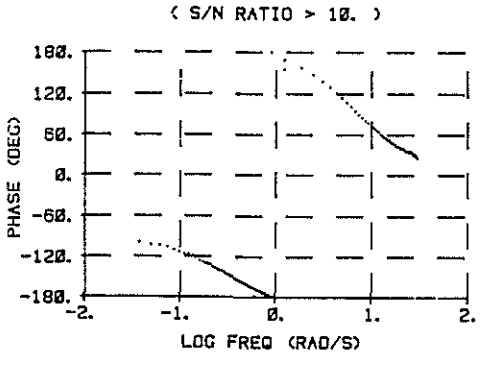

FIG. A.3 Sweep Response of the Lag Compensator